VALERI: a network of sites and a methodology for the validation of medium spatial resolution land satellite products

Frédéric Baret, Marie Weiss, Denis Allard, Sébastien Garrigue, Marc Leroy, Hervé Jeanjean5, R Fernandes, R Myneni, J Privette, J Morisette, et al.

VALERI: a network of sites and a methodology for the validation of medium spatial resolution land satellite products

Frédéric Baret[1], Marie Weiss[2], Denis Allard[3], Sébastien Garrigue[1], Marc Leroy[4], Hervé Jeanjean5, R. Fernandes, R. Myneni, J. Privette, J. Morisette Hervé Bohbot[6], Roland Bosseno[7], Gérard Dedieu[8], Carlos Di Bella[9], Benoit Duchemin, Marisa Espana[10], Valery Gond[11], Xing Fa Gu[1], Dominique Guyon[12], Camille Lelong[13], Philippe Maisongrande[8], Eric Mougin[8], Tiit Nilson[14], Frank Veroustraete[15], Roxana Vintilla[16]

[1]INRA-CSE, Agroparc, 84914 Avignon, France
[2]NOVELTIS, Ramonville Saint Agne, France
[3]INRA, Biométrie, Agroparc, Avignon, France
[4]MEDIAS-France, Toulouse, France
[5]CNES, Toulouse, France
[6]CEFE, Montpellier, France
[7]IRD, INRA-CSE, Agroparc, Avignon, France
[8]CESBIO, Toulouse, France
[9]INTA, Castelar, Buones Aeres, Argentina
[10] Universidad Michoacana de San Nicolas de Hidalgo, Morelia, Mexico
[11]CIRAD, Laboratoire Régionale de Télédétection, Cayenne, French Guyana
[12]INRA bioclimatologie, Domaine de la grande ferrade, France
[13]CIRAD, maison de la télédétection, Montpellier, France
[14]Tartu Observatory, Tartu, Estonia
[15]VITO, Mol, Belgium.
[16]ICPA, Bucharest, Romania

ABSTRACT -

Validation is mandatory to quantify the reliability of satellite biophysical products that are now routinely generated by a range of sensors. This paper presents the VALERI project dedicated to the validation of the products derived from medium resolution satellite sensors (www. avignon.inra.fr/valeri/). It describes the sites used, and the methodology developed to get the high spatial resolution map of the biophysical variables considered, i.e. *LAI*, *fAPAR* and *fCover* that can be estimated from ground level gap fraction measurements.

Sites were selected to represent , with the other validation projects, the large variation of biomes and conditions observed over the Earth's surface. Each site is about 3×3 km² in size and should be flat and relatively homogeneous at the medium resolution scale. For each site, the methodology used to generate the high spatial resolution biophysical variable maps is described. It is mainly based on concurent use of local gound measurements and a high spatial resolution satellite image, generally SPOT-HRV. Local ground measurements should be representative of an elementary sampling unit (ESU) that has approximately the same size as a SPOT-HRV pixel. The ground measurements mainly consist of gap fraction measurements achieved with LAI-2000 or hemispherical photographs. The ESUs are selected over the whole 3×3 km² site in order to sample the range of vegetation types observed. A transfer function is subsequently established over the ESUs to relate the ground measurements of the biophysical variables considered to the correspodonding high spatial resolution satellite image data. Finally, co-kriging is applied to generate the high spatial resolution map of the biophysical variables over the 3×3 km² area.

The methodology presented in this paper can serve as a basis for validating medium resolution satellite products. These methodological aspects are discussed and conclusions drawn on the limitations and prospects of beforementioned validation activity.

Key-words: remote sensing, biophysical variable, validation, kriging, upscaling, transfer function

1 INTRODUCTION

Medium spatial resolution satellite sensors operating in the solar domain (400-2500 nm) offer a unique way to monitor terrestrial surfaces over regional to global scales. Several applications are already using these data on an operational basis. They span over three main categories of users, namely, the scientific community, public institutions such as governments or international organisations, and private companies. Table 1 lists the users and their specific objectives along with the corresponding satellite products required, the associated spatial resolution and scale, information update period and duration of time series of observations. This table results from a compilation of several documents including those derived by international initiatives such as IGOS (Cihlar, Denning et al. 2000), GTOS (Heal, Menaut et al. 1995), (Cilhar, Denning et al. 2000), IGBP (Belward, Estes et al. 1999), ((NOAA) 1997), as well as the reports issued for the preparation of present and future medium resolution missions (POLDER, VEGETATION, MODIS, MISR, NPOESS, GLI, MERIS, MSG, AVHRR). It illustrates the wide range of use and order of magnitude of the spatial and temporal sampling associated to the observations.

As satellite products, both quantitative (the biophysical variables such as *fAPAR*, *fCover*, albedo, chlorophyll content and *LAI*) and qualitative or relative information (*VI* and classification) are required:

- ***Land use*** : Classification techniques applied for land use mapping will not be discussed here since it is not the main focus of this paper. However, the use of seasonality derived from a biophysical variable time course can improve the classification process,
- ***Albedo:*** is the main term for energy balance models of the Earth's surface. It corresponds to the amount of energy scattered by the surface in all upward directions and integrated over the whole spectrum (Jacob, Weiss et al. 2002). Albedo depends on the irradiance conditions as well as location (latitude) and date considered. It is generally decomposed into white and black sky quantities (Wanner, Strahler et al. 1997).
- ***fCover:*** the cover fraction simply describes the amount of vegetation. It is also generally related to the green parts of the canopies. This variable intervenes in a range of processes, and governs the partition between soil and vegetation contribution for emissivity, temperature and evaporation. It does not depend on latitude and date as opposed to *fAPAR* and albedo.
- ***fAPAR:*** the fraction of photosynthetic active radiation absorbed by a canopy is used as main input in net primary production models describing photosynthesis and thus the carbon budget. Only the green parts which are the only ones directly involved in photosynthesis processes should be considered. *fAPAR* is generally integrated over the diurnal course and depends thus on the corresponding irradiance conditions.
- ***LAI***: the leaf area index is the main driver of most canopy functioning and SVAT models since it represents the acual size of the interface between the canopy and the atmosphere. The leaf area index should be defined here as the area of the green leaves (one sided) per unit of horizontal soil (Privette, Morisette et al. 2001).
- ***Chlorophyll content***: This biophysical variable computed at the canopy level is linked to the nitrogen status that strongly influences photosynthesis and respiration processes. It can be considered as the terrestrial counterpart to chlorophyll concentration in oceanic phytoplankton.
- ***Vegetation indices (VI)***: a large variety of vegetation indices have been designed to monitor vegetation amount while minimizing the effect of confounding factors such as soil background, atmosphere, topography or geometry of observation. They consist of relatively simple combinations of reflectance observed in few wavebands. However, in most cases, they are not strictly linked to a particular biophysical variable, and can not be considered as a true biophysical variables. Nevertheless, good relationships are generally found between *fAPAR*, *fCover*, *LAI* and a *VI* within restricted set of conditions. Except when assigning a precise meaning to the 'vegetation amount' that *VIs* are targeting, *VIs* can not be properly optimized, neither rigorously evaluated or validated. For this reason, it is preferable to characterize vegetation amount by a given biophysical variable. The cover fraction, *fCover*, is a good candidate since it is relatively easy to estimate as compared to *LAI*. In addition, *fCover* is almost scale invariant, and independent of illumination conditions such as albedo or *fAPAR*.

This brief description of the products required by users of medium resolution satellite data, stresses the importance of biophysical variables such as *fCover*, *fAPAR*, *LAI* and albedo that can ultimately replace the current use of vegetation indices. The spatial resolution required ranges between 0.1 to 10 km, although there are not too many strong arguments to specify an optimal value. These values come partly from the analysis of the current applications of medium resolution sensors and are certainly biaised. However, they strictly depend on the use considered, as well as on the spatial heterogeneity of the landscapes and the non linearity between reflectance and the biophysical variable considered (Becker and Li 1995) (Raffy, Soudani et al. 2003). From this point of view, the scale effect will be quite important for *LAI*, and chlorophyll content (Weiss, Baret et al. 2000),

marginal for *fAPAR* and *fCover* (Malingreau and Belward 1992) (De Fries, Townshend et al. 1997; Weiss, Baret et al. 2000), and neglectable for albedo which is directly linked to a radiation flux quantity that is measured from satellite reflectances. From these arguments, it is relatively straightworward to conclude that relatively high spatial resolution (few tenths of meters), allowing global and frequent coverage (better than 10 days information update) would be more than welcome for most of the applications listed in Table 1!

Type of Users	Users	Objectives	Products							Reso-lution			Scale		Information up-date period (days)	Duration of observations (years)
			Land cover	VI	fCover	fAPAR	albedo	LAI	Chlor. Cont.	0.1 km	1.0 km	10 km	regional	global		
Scientific	Scientific community involved in global change studies including climate, green house gases	Identification of inter-annual climate and vegetation trends		X	X	X			X		X	X		X	10-30	>10
		Modeling canopy functioning within Earth system models	X	X	X	X		X	x		X	X	X	X	10	10
		Monitoring land cover change	X							X	X	x	X	X	10-30	>5
		Modeling ecosystem dynamics	X		X	X		X		X	X		X		10-30	>10
	Scientific community involved in Hydrology and water cycle studies	Quantitative vegetation monitoring	X		X	X	X	X	X	X	X	X	X	X	10	>10
Public	Early warning systems (GIEWS, FEWS)	Vegetation monitoring with comparison to a reference time course		X	X	X			X		X		X		10	>10
	pest risks evaluation (locusta, rift valley fiever, …)	Characterization of pests biotas, epidemiology	X		X	X		X		X	X		X		10	>10
	Meteorological organisations operating NWP (ECMWF, …)	Definition of the surface scheme	X		X		X	X			X	X	X	X	10	Cont[1].
	Operationnal agrométéorological systems (Agrhymet, …)	Production and productivity estimation	X	x		X		X	X		X		X		10	>10
	Desertification and deforestation monitoring (UNEP / FAO,)	Quantitative monitoring of vegetation	X		X			X	X	x	X		X	X	10	
	Governments for the implementation and verification of international treaties (Kyoto, …)	Monitoring land cover change	X							X	X	X	X	X	10-30	>10
		carbon sources and sinks	X			X	X	X	X	X	X	X	X		10	Cont[1].
Private	International agriculture and forestry companies, Insurance companies, Traders	Conjoncture analysis: phenology and change detection			X	X		X	x		X		X		10	>10
		Evaluation of the land use	X							X	X		X		10-30	5
		Maping risk/damage levels (fire, pests, flooding, drought, …)	X			X		X	X	X	X		X		10	>10
		Production estimates	X			X		X	X	X	X		X		10	>10

Table 1. Satellite data users, and the associated specific objectives and satellite products required. The X correspond to requirement in terms of product type, spatial resolution and scale, information update period and duration of time series of observations.

Table 1 shows that the duration of observations needs to be either continuous for operational meteorological services, or requires past time series of 5 to more than 10 years. Such long term studies allow to build a reference profile accounting for climate fluctuations, and to detect changes when the trend is subtle (Myneni, Keeling et al. 1997). The expected period for information updates is around 10 to 30 days, mainly governed by vegetation dynamics that can be very fast for some biomes and seasons (Gond, de Pury et al. 1999). To fulfill these conditions, three requirements have to be combined:

- ***to ensure the continuity of satellite observations.*** This is actually the case since the first launch of AVHRR in 1981, with a multiplicity of sensors since 1997 with ATSR, POLDER/ADEOS, VEGETATION, SEAWIFS, MODIS, MISR and MERIS. For the future, the space agencies are planning to launch new sensors to ensure the continuity of such global observations.
- ***to develop algorithms allowing the derivation of biophysical products in a consistent way*** from the past, current and future satellite sensors. The quality of the products should also be assessed with respect to their uncertainties that will vary with the sensor or combination of sensors used. There is currently no consensus on an algorithm and they thus have to be evaluated and compared. It is possible that for some specific applications, process models will assimilate directly the radiance values. However, in this case, the validation of the intermediate products is also mandatory to make sure that the models used and the assimilation procedure are properly implemented and pertinent.
- ***to validate the products and provide estimates of uncertainties.*** The validation is the process of assessing by independent means the accuracy of data products derived from the system outputs (Justice, Starr et al. 1998). This will provide the confidence intervals that is mandatory in a number of applications, including those based on a data assimilation approach.

This study focuses on the validation activity in the framework of several projects that are currently developed (Justice, Belward et al. 2000). (Justice, Starr et al. 1998; Privette, Myneni et al. 1998; Justice, Belward et al. 2000; Morissette, Privette et al. 2000; Weiss, Baret et al. 2000; Privette, Morisette et al. 2001; Baret, Weiss et al. 2002; Chen, Pavlic et al. 2002; Duchemin, B. et al. 2002; Liang, Shuey et al. 2002; Tian, Woodcock et al. 2002; Tian, Woodcock et al. 2002; Weiss, Baret et al. 2002). They are coordinated within the Commitee on Earth Observation Satellites (CEOS) by the Working group on Calibration and Validation (WGCV), sub-group on Land Product Validation (LPV) in order to get consistent approaches and to use in a synergistic way the data gathered by individual teams. The validation projects aim at providing high spatial resolution maps (order of 10-50 m) of the biophysical variables of interest over a network of sites covering a wide range of vegetation types and conditions.This high spatial resolution map could then be exploited by agregation of the data to the proper satellite resolution to provide the independent ground truth for the validation.

This paper focuses on the VALERI project (Validation of LAnd European Remote sensing Instruments) for which a proper methodology is proposed to generate the high spatial resolution map of the biophysical products. Therefore the final step of the validation exercise is not addressed here. It consists to compare biophysical values agregated at the scale of the medium spatial resolution sensors and derived from ground measurements to those of the corresonding satellite products. This final step of the validation will be presented within future papers.

This article describes the network of sites and the methodology that is illustrated by actual results. As a matter of fact, the methodology has evolved since the beginning of the project in 2000. The methodology presented here after is now almost stabilized and considered to be mature enough to be applied on a routine basis for such validation activity. VALERI mostly focused on products that can be derived from simple gap fraction measurements, i.e. *fCover*, *fAPAR* and *LAI.*

THE NETWORK OF SITES

The selected sites must fulfill a number of criteria to enable the provision of accurate estimates of biophysical variables from ground measurements.

Size: The spatial resolution of the sensors considered ranges from few hundred of meters (MODIS, MERIS) to a few kilometers (MSG) with most of the sensors being around 1 km² (AVHRR, VEGETATION, SEAWIFS). Therefore, the validation sites must cover at least a 3×3 km² area. Larger sites would be ideal for even coarser resolution sensors such as POLDER. However, the corresponding resources required for characterizing such a large site would be too high. As an alternative, products derived from POLDER can be evaluated by comparison with other sensors products or over spatially homogeneous areas.

Homogeneity: it should be relatively homogeneous, i.e. the biophysical variable value as well as the corresponding radiometric values may change only marginaly when shifting the position of a 1km² pixel within the 3×3 km² square.

Topography: the area should be relatively flat to simplify the interpretation both of the ground measurements and the satellite data.

Biome type: the selection of sites is made in order to sample the variability of biomes and conditions encountered over the Earth's surface. Obviously this is also governed by the availability of local support for the measurements. Furthermore, the VALERI activity is coordinated with that of other validation initiatives such as that NASA's MODLAND, CCRS LAI validation activity (Chen, Pavlic et al. 2002), (Privette, Myneni et al. 1998), (Morissette, Privette et al. 2000) (Fernandes, Burton et al. 2003) through the CEOS.

Num	Site	Country	Lat. (°)	Long. (°)	Date	FAO Biome Type	NDVI
1.1	AekLoba	Sumatra	2.63	99.58	04/01	Broadleaf Forest	0,65 (0,04)
2.1	Alpilles	France	43.81	4.74	03/01	Cropland	0,41(0,19)
2.2					07/02		0,38 (0,15)
3.1	Barrax	Spain	39.06	2.10	07/03	Cropland	0,28 (0,19)
4.1	Concepcion	Chile	-37.47	-73.47	04/03	Needle leaf forest	0,69 (0,09)
5.1	Counami	French Guyana	5.35	-53.24	09/01	Broadleaf Forest	0,69 (0,03)
5.2					10/02		
6.1	Fundulea	Romania	44.41	26.58	03/01	Cropland	0,59 (0,16)
6.2					05/01		0,62 (0,23)
6.3					05/02		
6.4					05/03		
7.1	Gilching	Germany	48.08	11.33	07/02	Mixed forest	0,60 (0,12)
8.1	Gourma	Mali	15.32	-1.55	09/00	Savanna	0,22 (0,01)
8.2					09/01		
8.3					09/02		
9.1	Haouz	Morocco	31.66	-7.60	03/03	Cropland	
10.1	Hirsikangas	Finland	62.64	27.01	08/03	Needle leaf forest	0,60 (0,10)
11.1	Jarvselja	Estonia	58.29	27.29	07/00	Mixed forest	0,63 (0,06)
11.2					07/01		0,70 (0,06)
11.3					07/02		
11.4					07/03		
12.1	Laprida	Argentina	36.99	-60.55	11/01	Grassland	0,62 (0,09)
12.2					11/02	Grassland	
13.1	Larose	Canada	45.38	-75.22	08/03	Mixed forest	0,70 (0,06)
14.1	Larzac	France	43.95	3.12	07/02	Grassland	
15.1	Nezer	France	44.57	-1.04	07/00	Needle leaf forest	0,44 (0,11)
15.2	Nezer				04/01		0,61 (0,11)
15.3	Nezer				06/01		0,54 (0,09)
15.4	Nezer				04/02		0,45 (0,10)
16.1	Puechabon		43.72	3.65	06/01	Closed Shrubland	0,54 (0,10)
17.1	Romilly	France	48.45	3.94	06/00	Cropland	0,63 (0,14)
18.1	Sierra_Cincua	Mexico	19.67	-100.28	12/01	Needle leaf forest	0,52 (0,15)
19.1	Sud_Ouest	France	43.51	1.24	07/02	Cropland	0,52 (0,16)
20.1	Turco	Bolivia	-18.23	-68.18	07/01	Baren & Sparsely Veg.	0,11 (0,02)
20.2	Turco				08/02		0,11 (0,01)
20.3	Turco				04/03		0,13 (0,02)
21.1	Zhang_Bei	China	41.29	114.69	08/02	Grassland	
22.1	Gnangara	Australia	116.11	32.37	03/04	Broadleaf Forest	

Table 2. Description of the sites sampled within VALERI. The NDVI values computed on the 3×3km² from the SPOT-HRV reflectance (TOA) is given, with standard deviation in parenthesis. The biome types correspond to the 17 FAO land cover classes.

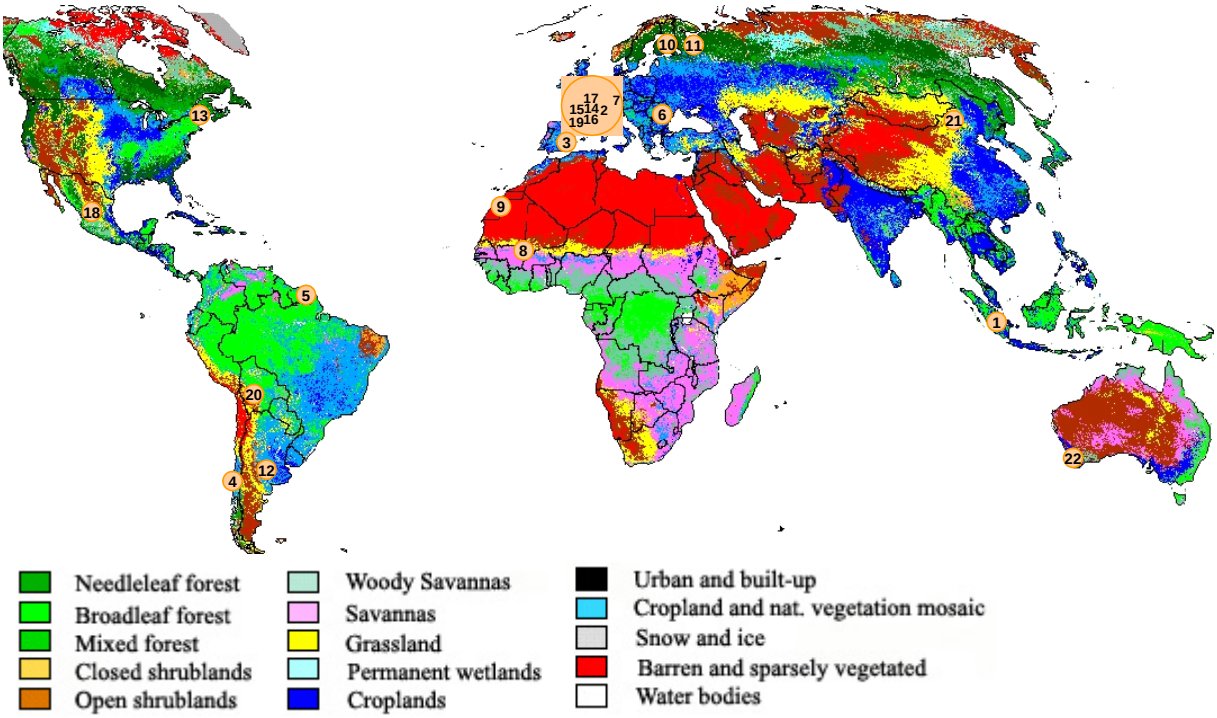

Figure 1. Map of the VALERI sites and those of other validation activities. The 17 FAO classes are represented (deciduous and evergreen forests are merged together). This classification was produced by VUB and Vito, with the support of OSTC using VEGETATION data (www.geosuccess.net/Geosuccess).

FAO Cover Classes	VALERI sites	Total Validation sites	% Total sites	% FAO vegetation Classes
Needleleaf forest	7	24	35.3	6.4
Broadleaf forest	4	10	14.7	11.9
Mixed forest	6	31	45.6	4.9
Closed shrublands	1	1	1.5	2.0
Open shrublands	0	4	5.9	14.0
Woody savannas	0	3	4.4	7.9
Savannas	3	5	7.4	7.2
Grassland	4	10	14.7	8.6
Permanent wetlands	0	0	0.0	1.0
Croplands	10	16	23.5	10.8
Cropland & natural vegetation mosaic	0	0	0.0	10.8
Barren and sparsely vegetated	3	3	4.4	14.4
TOTAL	**38**	**107**	**100.0**	**100.0**

Table 3. Number of sites sampled per biome type. The VALERI sites and the sites from the other initiatives (EOS/NASA, CCRS, and others) are separated. "% Total sites" is the number of sites sampled (VALERI and others) for each biome class divided by the total number of sites sampled over all the biome classes. The fraction of land area represented by each class is also given for comparison (data coming from (Loveland, Reed et al. 2000).

The distribution of the VALERI sites around the globe (Figure 1 and Table 2) shows that the main biomes are sampled, except the "Cropland and natural vegetation mosaic" that represents almost 10% of the global land surface and the "Permanent wetlands" which are not globally very important surface wise (Table 3). The difficulty to validate medium spatial resolution satellite products over heterogeneous landscapes explains certainly why the "Cropland and natural vegetation mosaic" class was not investigated up to now. The "Open shrublands" and "Woody savannas" that are not yet sampled within VALERI were sampled by other validation activities as shown in Table 3. It shows also that the "Needleleaf forests" and "Mixed forests" are much more sampled than the other biomes. This results mainly from the intensive Canadian activity that holds since 1994 mainly over Boreal forests (Chen, Pavlic et al. 2002). The classes corresponding to low vegetation amounts are

relatively undersampled with only one site for ”Open shrublands”, “Woody savannas” and “Barren and sparsely vegetated”.

The distribution of the NDVI values (Table2) within VALERI shows also that the higher NDVI values are more frequently sampled. This can partly be explained by the sampling period, that was generally close to the maximum vegetation amount.

The design of the global sampling strategy should also be oriented by the user requirements. However, conflicts will rapidly occur between different applications: carbon cycle applications will certainly put the emphasis on forests, whereas food security applications will focus on crop- and grasslands, and desertication investigations will obviously focus on sparsely vegetated areas. All these coniderations will have to be accounted for in the future selection of the VALERI validation sites. Furthermore, the evaluation of the uncertainties associated with the validation activity will be assessed by repeated observations over sites corresponding with almost steady vegetation. For this reason, few sites are sampled several time (Nezer, Counami, Järvselja) to check the consistency of the ground estimates of the biophysical variables scaled up to medium spatial resolution sensors.

THE METHODOLOGY APPLIED ON EACH SITE

Overview

A dedicated methodology has been developped to set a consistent framework for the validation exercise. It is based on the concurrent use of a high spatial resolution satellite image and ground measurements. As opposed to the methodology based on patches of landscape elements as proposed by (Tian, Woodcock et al. 2002) for the validation of MODIS products, the VALERI approach is based on clusters of local measurements that aim at representing a small group of pixels of the high spatial resolution satellite image. These clusters are called ‘Elementary Sampling Units’ (ESUs). A series of ESUs is distributed over the whole 3×3 km² site to sample the variability in vegetation structure. A transfer function is then calibrated over the ensemble of ESUs to relate the biophysical variable measured to the corresponding high spatial resolution radiometric data. This transfer function, once calibrated over the ESUs, could then be extended over the whole site using the high spatial resolution image. In order to take advantage of all available information, co-located kriging is applied (Goovaerts 1997). This allows to both account for the measurement points and for the previously generated high spatial resolution image. Figure 2 sketches the approach used. In the following, we will present and discuss the different steps of this methodology.

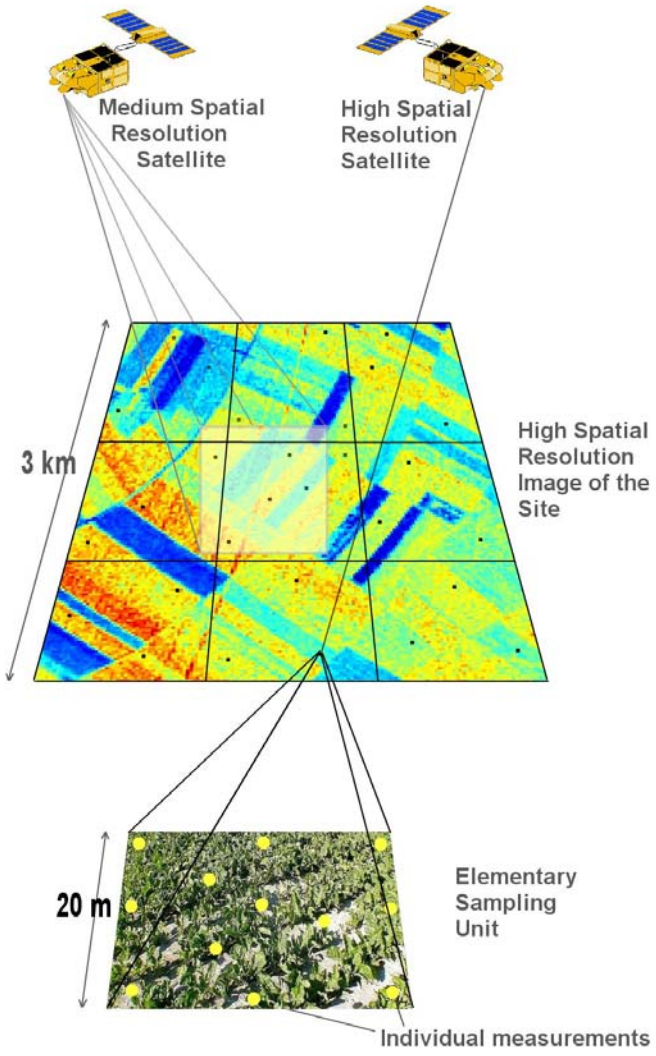

Figure 2.: Scheme describing the strategy used to derive the biophysical maps at high spatial resolution from the combination of the individual ground measurements (the yellow spots) performed over the Elementary Sampling Units (ESUs) and the high spatial resolution satellite images over the whole 3×3 km² site. The medium spatial resolution satellite pixel is represented in faded colors.

Spatial sampling strategy for the whole 3×3 km² site

The objective here is to set the minimum number of ESUs at the optimal location both to (i) establish robust relationships between the measured biophysical variables and the corresponding high spatial resolution radiometric values over the ensemble of ESUs, and to (ii) get a good description of the geostatistics of the biophysical variable considered over the whole site. For these reasons, the site is divided into nine 1 km² squares, to get a more even distribution of the ESUs over the site, improving the estimation of the geostatiscal characteristics at this scale. Subsequently, in each 1 km² square, 3 to 5 ESUs are considered. Their location is chosen to globally sample equally in proportion all the cover types present in the whole site as well as the variability within each cover type. In addition, two constraints have to be accounted for: first the ESUs have to be close to an access (road, path, …) for more conveniency, but far enough from a landscape boundary to minimize the possible contamination of the radiometry of the considered ESU due to the misregistration between the GPS geolocated ESU and the corresponding high spatial resolution image. Second, the ESUs should also be ideally spread spatially equal within the 1km² square to improve the geostatistical variables estimation. Furthermore, the 1 km² square that is located at the centre of the WS should be more densely sampled (between 5 to 7 ESUs) for a better description of the geostatistics for the medium range lags.

This proposed scheme leads to a total number of 30 to 50 ESUs to sample the whole site. Considering the size of ESUs (around 20×20 m²), the sampling rate of the WS ranges between 0.13% and 0.22%. Depending on the type of instruments used for the local measurements of the biophysical variables, and the difficulty to access the ESUs, the required manpower is between 4 man-days (2 teams of 2 people for one day) to 20 man-days. Ideally the measurement period should not exceed one week, otherwise the vegetation might significantly evolve.

Once the high spatial resolution image is acquired, the quality of the sampling is evaluated based on the simple *NDVI* distribution. Ideally, the distribution of *NDVI* values of the *ESUs* should be close to that of the whole site. However, because the size of the sample is drastically different for the ESUs (between 30 to 50) and for the whole site (22500 in the case of a 3x3km² SPOT image), it is not statistically consistent to directly compare the two *NDVI* histograms. Therefore, we proposed to compare the *NDVI* cumulative frequency of the two distributions by:

1. Computing the cumulative frequency of the *NDVI* values of the 30 to 50 ESUs.
2. Applying a given translation to all of the 50 pixels (modulo the size of the image).
3. Computing the cumulative *NDVI* frequency of the new set of translated pixels.
4. Repeating steps 2 and 3, 199 times with 199 random values of the translation vectors.

This provides a total population of N=199+1(actual) cumulative frequency on which a statistical test at acceptance probability $1-\alpha = 95\%$ is applied: for a given *NDVI* level, if the actual ESU density function is in between two limits defined by the 5 ($\alpha/2.N = 5$) highest and lowest values of the 200 cumulative frequencies, the hypothesis that the two *NDVI* distributions are equivalent is accepted. Otherwise it is rejected and the results should be used with greater care.

Results obtained for the Alpilles site (Figure 3 left), show that the actual cumulative frequency is very close to the 5 lowest distributions, particularly for *NDVI* values between 0.3 and 0.5, as well as between 0.6 and 1. The sampling appears therefore not fully representative. However, the land cover shows that the surface that were not covered by vegetations were significant and were obviously not sampled by ESUs (roads, senescent wheat, bare soil, …). Therefore, it should be more sound to discard in the sampling strategy these areas where the green *LAI* is known to be 0 (roads, houses, …) by applying masks on the images for such land cover types. Conversely, for the 2001 Puechabon site (Figure 3 right), the sampling was satisfactory since a relativey large number of ESUs were sampled.

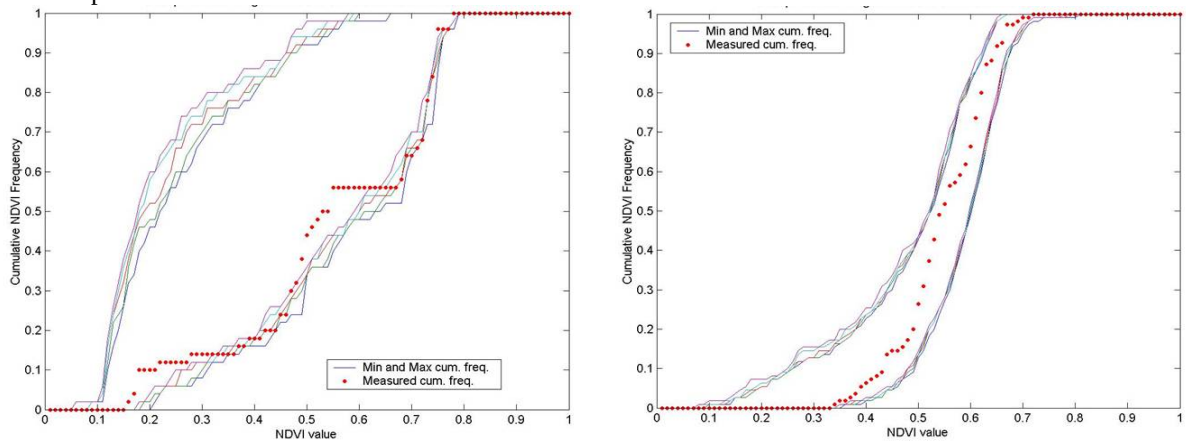

Figure 3. Illustration of the test applied to verify the representativeness of the ESUs. The figure on the left correponds to the Alpilles site. That on the right corresponds to Puechabon site. If the NDVI distribution (the dots) are in between the 5 minimum and maximum cumulative distributions, then the ESU sampling is considered to be representative.

An additional method was also used to map the areas poorly represented by the ensemble of ESUs. The convex hull of the radiometric values of the high spatial resolution image is computed. Then, each pixel that falls outside this convex hull is flagged. This means that the biophysical variable of interest of any pixel that belongs to the radiometric convex hull, could be interpolated from the values of the ESUs. This is not the case for pixels outside the convex hull, where the estimation of the corresponding biophysical variable will be based on extrapolation of the values of the ESUs. Extrapolation of empirical relationships should always be handled with great care. Figure 4 shows an example of such maps.

Figure 4. Maps of the pixels flagged because they were outside the radiometric convex hull.

Local estimation of the biophysical variables over the elementary sampling units

Depending on the features of canopies, two types of measurements are performed at ground level on the ESUs to estimate *LAI*, *fAPAR* and *fCover*. If the vegetation can be considered as homogeneous (at the ESU scale), the estimation is made using gap fraction measurements following cross or square spatial sampling (Figure 4). A detailed study not presented here has shown that both sampling strategies are very similar. An alternative sampling scheme (transect in figure 4) is used when the vegetation is heterogeneously distributed within the ESU such as in the case of sparse canopies. Note that the area actually sampled might be larger than the original 20m

square for tall vegetation canopies such as forests. For a canopy of height *h* and maximum zenith angle used θ_{max}, the actual side of the ESU would be 20+ 2.*h*.tan(θ_{max}). In the case of 30m forests and θ_{max} up to 60° the side of the ESU will be close to 125m!

Gap fraction measurements. The gap fraction is an integrated canopy structural quantity. The vertical gap fraction corresponds directly to the complement to unity of the cover fraction (*fCover*). The gap fraction in the sun direction provides a direct estimation of instantaneous *fAPAR* (Baret, Andrieu et al. 1993). However, dynamic vegetation models often require estimates of *fAPAR* integrated over the day. This can be achieved by estimating both the black-sky *fAPAR* (directional *fAPAR*) and the white sky *fAPAR* (diffuse *fAPAR* for a given sky luminance distribution often assumed isotropic) similarly to what is proposed for albedo (Martonchik 1994). Then, the daily integrated value can be derived from the knowledge of the variation of the diffuse fraction along the day, the sun position course and the corresponding incoming radiance. Finally, gap fraction measurements allow to estimate the *LAI* of canopies with an asumption about the spatial organisation of the vegetation elements. This principle is exploited by the LAI2000 instrument to estimate *LAI* that provides an estimate of effective *LAI*, i.e. assuming all the elements being green and randomly distributed. The same principle can be also applied to hemispherical photographs (e.g. (Chen, Black et al. 1991), (Leblanc, Fernandes et al. 2002). The use of color hemispherical photographs reduces the uncertainty associated to the green fraction estimation that is often significant for forest canopies (Fernandes, White et al. 2002). Hemispherical photography provides also information on the clumpiness through the gap size distribution (Chen and Cilhar 1995). This is the reason why hemispherical photographs are progressively replacing LAI2000 devices within the VALERI project. Furthermore, hemispherical photographs can be used in the case of low vegetation canopies by taking downwards looking photographs. They can also be used in more variable illumination conditions, particularly when looking upwards, which makes the measurements more flexible as compared to LAI2000. The latter requires stable diffuse illumination conditions. A dedicated software was developped to process these color photographs with emphasis on green element classification and processing of series of photographs (CAN-EYE www.avignon.inra.fr/can_eye). A more detailed review of the *LAI* estimation from gap fraction measurements is given by (Weiss, Baret et al. 2004) with special attention to the hemispherical photographs technique.

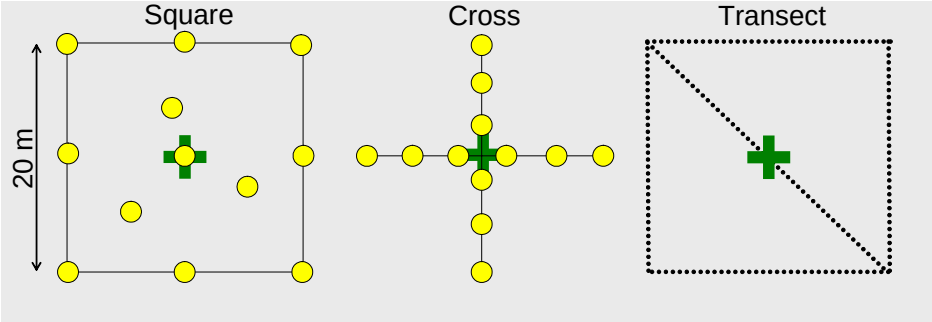

Figure 5.: The three spatial sampling schemes used to characterize an Elementary Sampling Unit. The small circles for the “square” and “cross” patterns represent the elementary points. The dashed lines for the “transect” pattern represent lines were measurements are performed at regular intervals and used for sparse canopies. The bold cross in the middle of each pattern represents the location of a GPS measurement.

The ESU is sampled by taking 12 measurements organized either in a “square” or “cross” patterns (Figure 4). The center of the ESU is geolocated using a non differential GPS that provides an accuracy typically around 5 to 10 m. Each elementary point is sampled by one LAI2000 or hemispherical photograph (Weiss, Baret et al. 2004). The “cross” pattern was originally designed to get geostatistical information for the short distances. However, it has been shown by simulations (results not presented in this paper) that the spatial sampling associated to the “square” pattern (Figure 4) leads to similar performances as that of the “cross”. The accuracy of the measurements was estimated to be close to 15% for effective *LAI* over crops.

Intersect measurements. For sparse and locally discontinuous vegetation, the above methods are not optimal, requiring a much denser sampling pattern. A variation of the general sampling scheme is proposed, based on the transects method (Buckland and Turnock, 1992). First, vegetation classes have to be defined for the whole site. Then, each ESU is sampled according to the “transect” pattern (Figure 5): the fractional cover for each vegetation class is estimated by the fraction of the line that intersects these vegetation classes. *LAI* is then assessed through destructive sampling of the representative vegetation classes considered. *fAPAR* could be estimated using hemispherical photographs performed at these locations.

Spatial extension of the ESUs to the whole site

The local measurements performed over the series of ESUs will be extended to the whole site using a dedicated process (Figure5) for which the different steps will be described in the following.

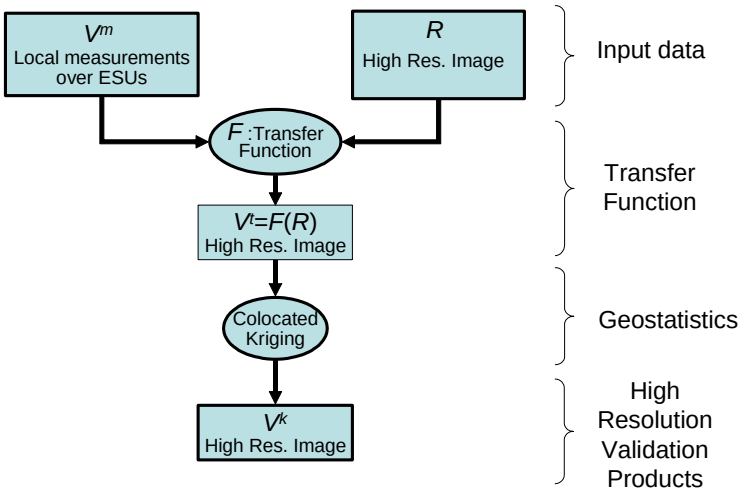

Figure 6.: Flow chart showing the way both high spatial resolution products are estimated from the combination of the ground measurements over the ESUs and the high spatial resolution image over the WS.

Development of a transfer function

The transfer function relates the high spatial resolution radiometric data to the corresponding ground measurements. It can be calibrated and evaluated over the ESUs, and subsequently applied to the whole site to derive a first version of the high spatial resolution map of the biophyisical products. Several types of transfer functions were investigated that can be either based on radiative transfer model inversion or purely empirical. The associated advantages and drawbacks will be discussed and illustrated over the Alpilles site.

Radiative transfer model inversion. The use of radiative transfer model inversion may lead to some circularity in the case of the validation of products that are derived from similar model inversion techniques applied at the medium spatial resolution. The comparison will be mainly indicative of the scaling problem, or of differences between the characteristics of the high and medium spatial resolution sensors (radiometric accuracy, atmospheric correction, bands and directions used). Nevertheless, the ground data can be here used to control the performances of the inversion process at the high spatial resolution. This validation approach was used for MODIS products (Tian, Woodcock et al. 2002). The comparison between to ground measurements over the ESUs provides also a correction that can be applied to the raw estimates by model inversion. This correction will be anyway achieved as we will see later, when applying the cokriging technique to the whole site.

Model inversion could be only applied if top of canopy reflectances are available, i.e. if an atmospheric correction was applied. This is unfortunately not always the case because in many situations the atmospheric properties were not measured during the high spatial resolution satellite overpass, and these satellites (mainly SPOT-HRV) offer only little possibility of autonomous atmospheric correction.

Figure 6 shows the result over the Alpilles site using SPOT-HRV as the high spatial resolution image. The calibrated top of atmosphere radiance were transformed into top of canopy reflectance values using the 6S model and the aerosol optical thickness as measured in the Avignon AERONET site (www.aeronet.com). The SAIL (Verhoef 1984; Verhoef 1985) coupled to the PROSPECT models (Jacquemoud and Baret 1990) were inverted using a look up table as described in detail by (Weiss, Baret et al. 2000). The range of variation of the input model variables are defined in Table 4, and the distribution laws are considered to be independent and uniform. The number of cases selected as the solution was optimised as well as the number of bands. It appears that using just the red and near infrared bands with 406 cases selected as the most probable solution over the 25000 simulated cases in the LUT, achieved the best performances evaluated using the RMSE values over the ensemble of ESUs. The corresponding estimated values of *LAI* assumed to be the median of the 406 best solutions were then corrected by applying a linear correlation with the measured reflectance values over the ESUs. This allows to remove any residual biase. The resulting RMSE value is 0.54 (Figure 6) as compared to 0.55 when the final linear correction was not applied.

Variable	Min	Max
LAI	0	6
ALA	40	85
HotSpot	0.01	1
Bsoil	0.5	3
Cab	20	100
Cdm (20%)	0.0025	0.0042
Cw (80%)	0.01	0.017
Cbp	0	0
N	1	2.5

Table 4. Range of variationof the input variables of the coupled SAIL and PROSPECT models used to generate the look up table exploited within the model inversion approach (for more details, see (Weiss, Baret et al. 2000)).

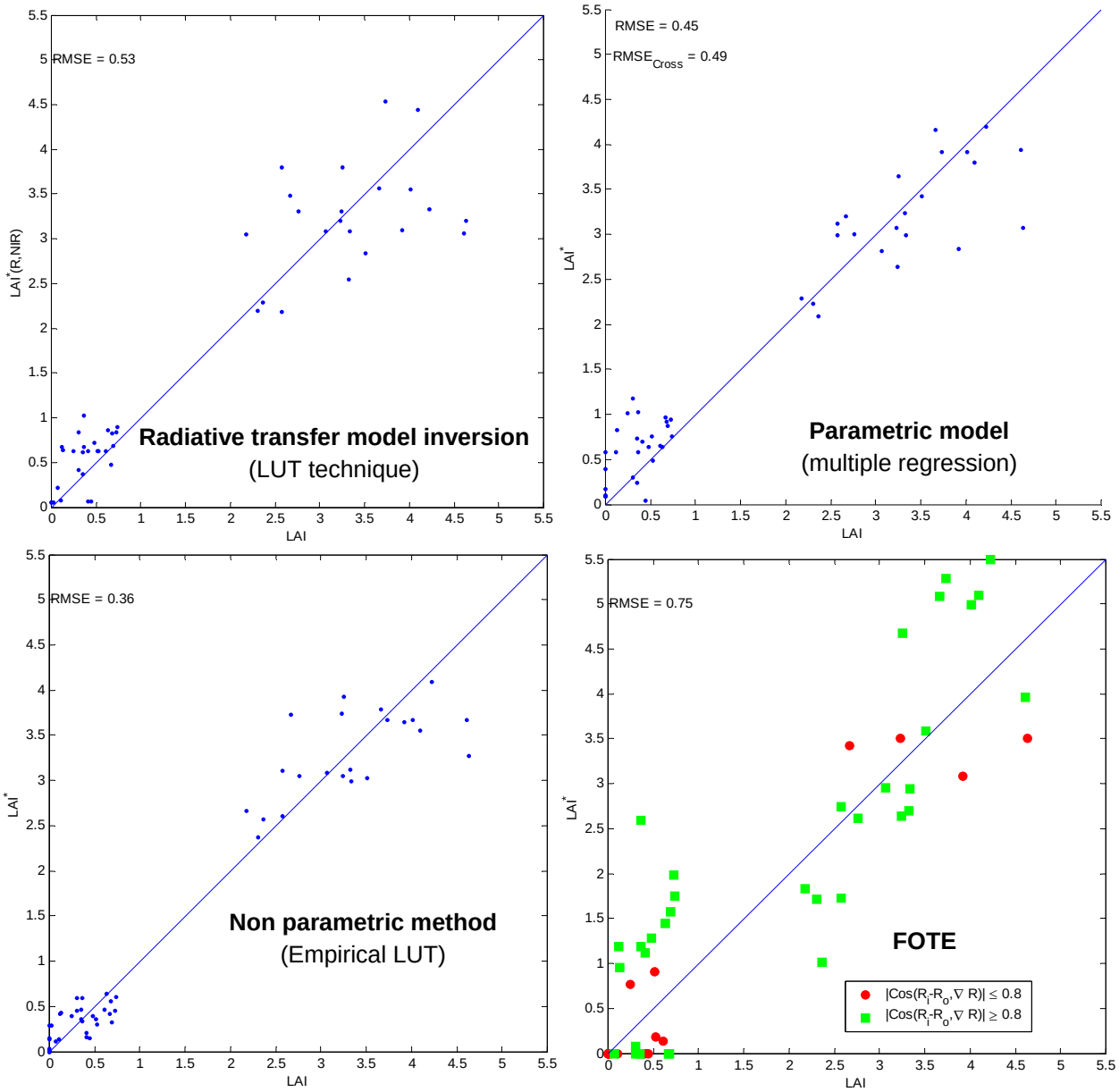

Figure 7. Comparison between the *LAI* values measured over the ESUs and those estimated through the several transfer functions. Results obtained over the Alpilles site in 2001. For the FOTE technique, the colinarity condition (equation 2) is indicated for each ESU.

Parametric model. This method consists to fit an empirical parametric model between the biophysical variable of interest as measured over the ESUs and the corresponding radiometric response. It thus allows to use raw radiance values from the satellite. It will generally provide good performances over the cover types sampled by the ESUs. In the case of sites with contrasted cover types, a segmentation of the image has to be performed, and the parametric model has to be calibrated for each main cover type. When a large number of cover types has to be considered, it may happen that for some of them the number of corresponding ESUs is low, and the internal variability sampled restricted. In these conditions, the fiting might have very little predictive capacities. This reenforced the importance of a well designed selection of the ESUs within the WS.

The empirical transfer function used are based on multiple linear regression but could also include the use of vegetation indices. The dependant variable is the ground measurement, and the independent variables are either the DC, radiances or reflectances, vegetation indices, or their logarithmic transforms. The uncertainty of the ground measurement for the dependant variable, and that associated to the radiometric noise and localisation effects are accounted for in the fitting of the parametric model. As a matter of fact, the GPS position is associated to an uncertainty, as is the geolocation of the high spatial resolution satellite pixels. These two positioning uncertainties translate into a radiometric uncertainty that will mainly depend on the local heterogeneity around the ESU.

Note that the method that consists in assigning to each class the corresponding mean measured *LAI* value computed over the ESUs belonging to this class, as used by (Tian, Woodcock et al. 2002) for MODIS validation, is a special case of this empirical fitting method with a nul slope and an offset equal to the average value of the ESUs. In the case of a unique class, this turns to be the most basic method, where the *LAI* value over the site is just computed as the average of all the *LAI* measurements over all the ESUs.

In the case of Alpilles site, a multiple linear relationship was established between the SPOT-HRV top of atmosphere radiometric data and the corresponding *LAI* as measured over the ESUs. Note that 10 additional ESUs corresponding to bare soil (LAI=0.0) were used in the development of the regression. Results (Figure 6) show that the RMSE was 0.45 when evaluated by cross-validation over the ESUs (without including the 10 bare soil additional ESUs). Comparison was also achieved with logarithmic transforms and vegetation indices, but the simple linear regression of the three top of atmosphere SPOT-HRV bands was performing the best.

Non parametric method. To avoid choosing a parametric model, and also partly to prevent from classifying the site into several vegetation types for which a dedicated parametric relationship has to be established, a non parametric method was investigated. It consists in generating a look up table over the ESUs made with the SPOT-HRV top of atmosphere radiometric data and the corresponding measured *LAI* values. Then, for each pixel of the whole site, its *LAI* value will be computed as the mean of the *n LAI* values corresponding to the ESUs having the closest radiometric response. The number *n* could be optimized over each data set investigated using cross validation techniques.

For the Alpilles site, the optimal value of the number *n* was found to be *n*=3. Note that, here again, the 10 additional bare soil ESUs were used in the generation of the empirical LUT. Results show (Figure 6) that this approach is performing the best with RMSE=0.36.

FOTE hybrid method. The advantages and limitations associated to the purely empirical and purely physical methods linked to the representativity of the ESUs have been discussed above and appear to be antagonist. To take advantage of these two types of approaches, an hybrid one is proposed. It assumed that, within a cover type, the radiometric values, ρ, of the high spatial resolution image is only governed by variations of the biophysical variable of interest, i.e. *LAI* in our case. The first order Taylor Element (FOTE) of the radiative transfer model *M* writes:

$$\overrightarrow{\rho_i} = \overrightarrow{\rho_o} + (LAI_i - LAI_o)\overrightarrow{\nabla\rho} \quad (1)$$

where $\overrightarrow{\rho_i}$ is the reflectance column vector of pixel *i* that contains *n* elements corresponding to the *n* bands of the high spatial resolution image, $\overrightarrow{\rho_o}$ is the average reflectance vector computed over the ESUs, $\overrightarrow{\nabla\rho}$ is vector of the derivatives of the reflectance with regards to the *LAI*. Equation (1) is only valid is the vectors $\left(\overrightarrow{\rho_i - \rho_o}\right)$ and $\overrightarrow{\nabla\rho}$ are collinear, i.e. if :

$$\begin{cases} \left\|\overrightarrow{\rho_i - \rho_o}\right\| = (LAI_i - LAI_o)\left\|\overrightarrow{\nabla\rho}\right\| * \mathrm{sgn}\left(\cos\left(\overrightarrow{\rho_i - \rho_o}, \overrightarrow{\nabla\rho}\right)\right) \\ \left|\cos\left(\overrightarrow{\rho_i - \rho_o}, \overrightarrow{\nabla\rho}\right)\right| = 1 \end{cases} \quad (2)$$

The vector of derivatives $\overrightarrow{\nabla\rho}$ could be computed as a numerical approximation of the derivatives of the radiative transfer model *M* around LAI_0:

$$\overrightarrow{\nabla\rho} = \left(\overrightarrow{\frac{\partial\rho}{\partial LAI}}\right)_{LAIo} = \left(\overrightarrow{\frac{M(LAI_o + \Delta LAI)}{\Delta LAI}}\right) \quad (3)$$

where ΔLAI corresponds to a small *LAI* variation.
Because of the basic assumption about the linearity between reflectance values and *LAI*, the method could only be applied over small range of *LAI* variations and for a given type of canopy. For this reason, a classification of the image must be first performed, and the FOTE method applied over each vegetation class.
The advantage of this method is to exploit concurrently both ground *LAI* measurements and radiative transfer modelling. It may be understood as correcting the mean *LAI* value of a given vegetation class as measured over some ESUs, by the difference observed in the reflectance signal, weighed by the sensitivity of the reflectance to *LAI*. By definition, the estimation should be unbiased. However, it requires top of the canopy reflectance values, i.e. calibrated reflectance corrected from the atmospheric effects. In addition, the method requires all the input variables of the radiative transfer model *M* to be known for the average case of the vegetation class considered. This is achieved by inverting *M* at point LAI_0 with the corresponding average reflectance $\overrightarrow{\rho_o}$ and LAI_0 values.
This method was also tested over the Alpilles site. A classification was first applied and six classes were identified. Then the SAIL model was inverted over the average reflectance values as measured over the ESUs belonging to each class. The corresponding derivatives vector $\overrightarrow{\nabla\rho}$ was computed. Finally, the image was obtained by applying equation (1) for each pixel of each class. Figure 6 shows that performances of this method are not very good (RMSE=0.75). This might be due to the strong assumption made on the fact that any variation of reflectance value is directly linked to a variation in leaf area index only. Figure 6 shows also that the colinearity condition (equation 2) is not always met.

In addition to the above evaluation over the ESUs, analysing the results applied over whole site allows to compare the robustness of these transfer functions (Figure 7). The radiative transfer model inversion shows the smoothest image with a resulting average *LAI* value of 0.97 for the whole site. The parametric model based on multiple linear regression shows the most crispy image with a *LAI* value of 0.90 for the whole site. This might come from the fact that any variation in reflectance will be translated in a *LAI* variation, as opposed to the radiative transfer model inversion technique that may not confound the effect of other canopy variables. The non parametric model shows more discrete patterns with the highest *LAI* values being slightly “eroded” resulting in a *LAI* value of 0.89 for the whole site. These three methods seemed relatively equivalent as opposed to the FOTE method that seemed more unstable particularly for the lowest values and the boundaries, leading to an average *LAI* value of 0.82 over the whole site.

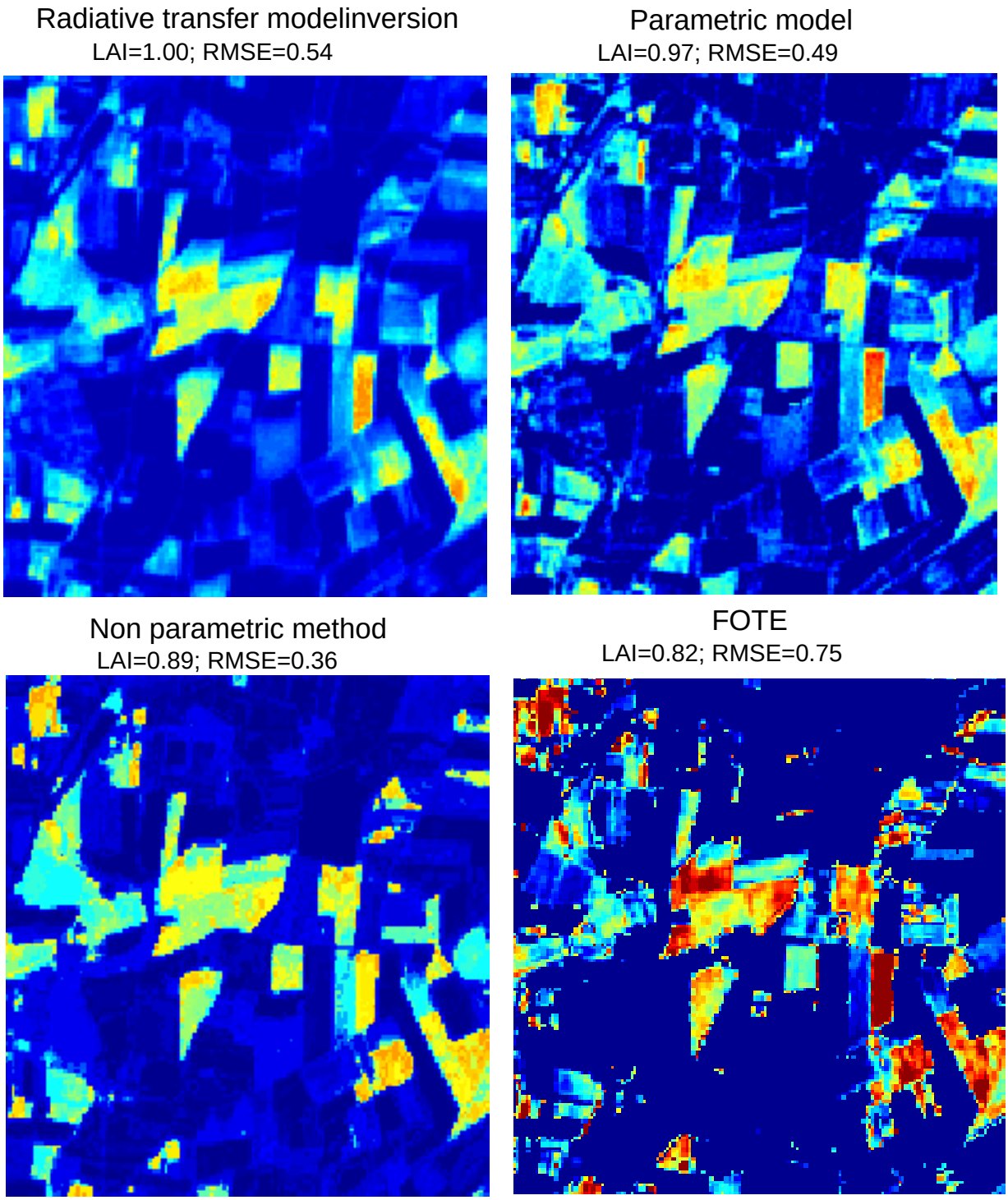

Figure 8. Maps of the *LAI* values over the Alpilles site as derived from the application of the several transfer functions. The mean LAI of the whole site is indicated along with the RMSE evaluated by cross validation over the ESUs.

The significant variation observed for the average *LAI* and also the *LAI* distribution indicate that the choice of the transfer function is critical. The evaluation over the ESUs as well as that obtained over the whole site, along with criterions based on the "independent" character of the validation exercise and the lack of characterization of the atmosphere would tend to select empirically based transfer functions. This selection of the best transfer function for the purpose of the validation exercise is further re-enforced by the fact that a significant time lag may exist between the ground measurements over the ESUs and the acquisition of the high spatial resolution image. The non parametric model is certainly a very appealing method that could implicitly account for the existence of different vegetation types within the ESU. However, in case of sites with bare soils and low vegetation amounts, it should be calibrated (similarly for the parametric model) by including some bare soil

"ESU" as implemented in this study to represent such objects. Its main limitation is however the very limited extrapolation capacity if areas of the site are not well represented, i.e. falling outside the radiometric convex hull.

Colocated kriging

Although the use of the transfer function allows to get a high spatial resolution image, the performances of the whole process highly depend on the accuracy of the transfer function. In case of poor transfer functions, or even in case of unavailable high spatial resolution satellite image, simple kriging techniques allow to get a back-up solution for the generation of the required high spatial resolution map of the biophysical variable. Colocated kriging technique allows to balance within a single formalism between these two extreme solutions for the generation of the high spatial resolution map of the biophysical variable (de Beaufort 2000). Colocated kriging technique is designed to estimate the value of a primary variable at any point in space from the knowledge of the measured values sampled over a limited number of points, and from the knowledge of the value of a secondary variable that is known at any point of the area investigated and that is linearly related to the primary variable (Goovaerts 1997). In our case, the primary variable is the biophysical variable of interest, *V*, that is measured over a limited number of ESUs. The secondary variable, *R*, is derived from the high spatial resolution image thanks to the transfer function *V(R)*. This way, the secondary variable should be linearly related to the primary variable and is an unbiased estimate of *V* knowing *R*. The kriged value $\hat{V}_i$ of the biophysical variable V_i at pixel *i* is built as a linear combination of the measured values *V* and the secondary variable *V*(*R*):

$$\hat{V}_i = \sum_{j=1}^{n} \lambda_j^i \cdot V_j + \delta_i \cdot V(R_i), \quad (2)$$

where *n* is the number of ESUs sampled within the cover type considered, V_j is the biophysical variable measured at the ESU *j*. The weights λ_j^i and δ_I are the solution of a linear system derived by minimizing the variance of the prediction error under the assumption of unbiasedness of the prediction error $E\left[\hat{V}_i - V_i\right]=0$ that leads to the constraint (Wackernagel 1995):

$$\sum_{j=1}^{n} \lambda_j^i + \delta_i = 1 \qquad (3)$$

Note that the simple kriging technique correspond to $\delta_i=0$, and the single use of the transfer function corresponds to $\lambda_j^i=0$. The weights λ_j^i and δ_i depend on the variogramme of *V* established over the ESUs, the sampling pattern, the location of the pixel *i* relative to the data and on the correlation coefficient between *V* and *V(R)*. If necessary, the variogram of the biophysical variable measurements is estimated thanks to the variogramme of *V*(*R*) computed on the high spatial resolution image. Note that it is important to correctly design the spatial sampling scheme for the ESUs to get a good estimation of the variogram at all distances as illustrated in Figure 8. For colocated kriging, it is assumed that the cross variogram is the product of the variogramme of the primary variable *V* and the correlation coefficient associated to the transfer function.

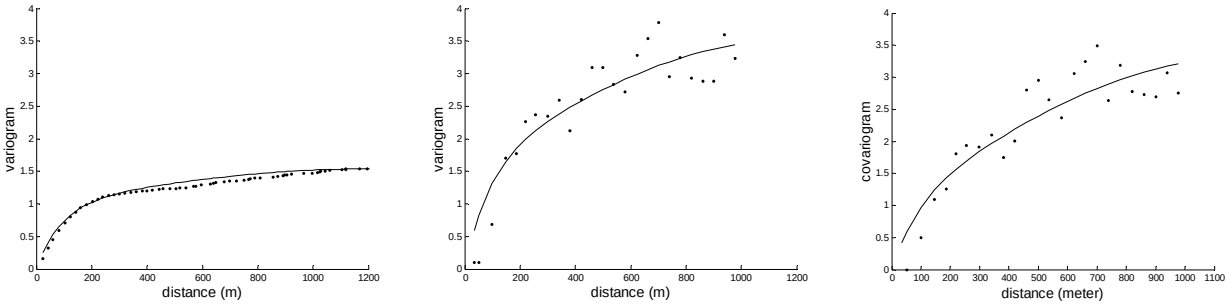

Figure 8. Variogrammes as observed over the Alpilles site in 2001. Solid line: model of theoretical variogram; dots: experimental variogram computed on the ESUs. The first one was computed over the high spatial resolution image of the biophysical variable derived by applying the transfer function to the original high resolution satellite image. The second one is obtained from the measurements over the ensemble of ESUs (the range was derived from that of the previous variogramme (estimated *LAI*)). The last one is the cross-variogramme (the range was derived from that of the first variogramme; the sill is computed as the product of the correlation coefficient associated to the transfer function with the sill of the estimated *LAI*).

Models of variogram can be evaluated by reestimating the data of each ESU using all other available data within a cross validation process. Results are presented in Figure 9 for three different models of variograms, for which the Root Mean Squared Error (RMSE) $\sqrt{1/n\sum_i\left(\hat{V}_i - V_i\right)^2}$ and the Root Mean Standardized Squared Error (RMSSE)

$\sqrt{1/n\sum_i \frac{(\hat{V}_i - V_i)^2}{\sigma_i^2}}$ are computed. The RMSE is a measure of the estimation performance. The RMSSE compares the squared error with the kriging variance given by the model. Results show that the exponential and spherical variogrammes lead to very similar performances, whereas the Kbessel variogramme performed poorer with over-optimistic kriging variance. Hence this model should be discarded.

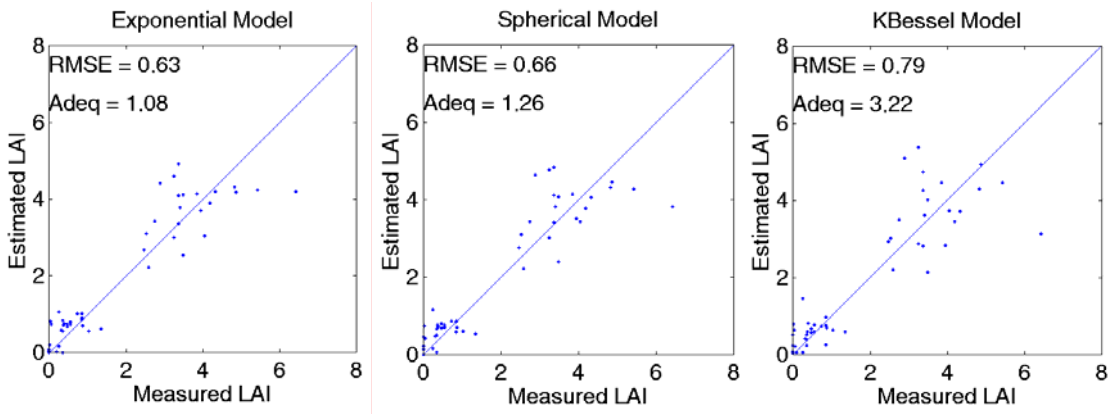

Figure 9. Comparison of the performances of three variogramme models (Exponential, Spherical and KBessel) applied on biophysical measurements over the ESUs as observed during Alpilles 2001. The evaluation is achieved by cross validation. RMSE is the root mean square error and RMSSE is the root mean standardized squared error.

Figure 10 shows a kriging map of the Alpilles site (2001) and a map of the weight δ. It is clearly visible that the radiometric information is generally the largest contributor to the local variable estimation, except in the very local vicinity of the ESUs where the contribution of the measured values over the ESUs dominates thanks to the strong but local spatial correlation. This demonstrates the interest of the colocated kriging technique that allows to account for the local measurements over the ESUS that represent generally a relatively local area, and the transfer function that allows to estimate the biophysical variable of interest at the longer distances thanks to the high spatial resolution satellite image and the transfer function.

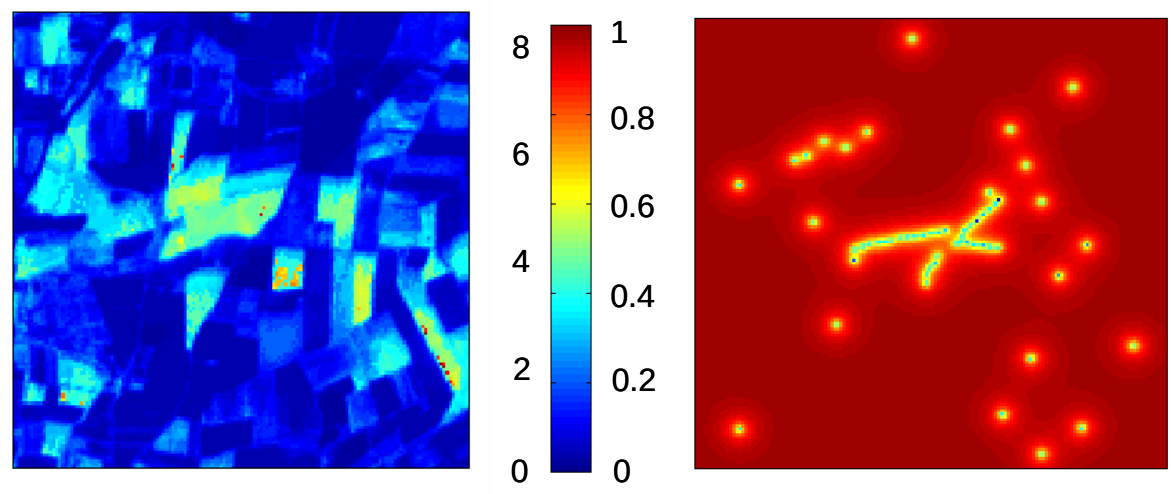

Figure 10. Co-located kriging applied to the Alpilles site (2001). The figure on the left represents the estimated LAI map. That on the right represents the weight δ associated to the radiometric information from the high spatial resolution image. The ESUs are associated to the lowest values of weights δ The lowest values of the weights δ are located near ESUs. Note that for this site, two transects of ESUs were sampled in the middle of the site.

The uncertainty associated to the prediction at pixel *i*, provided by the variogram model is evaluated by the kriging variance. It is the minimum variance of the prediction error,

$$\sigma_i^2 = Var\left(\hat{V}_i - V_i\right). \qquad (4)$$

Figure 11 shows the kringing variance map. We observed that the kriging variance is strictly null at the location of the ESUs. The largest values are obtained at a distance larger than 250m corresponding to the range of the variograms. We note that this kriging variance map looks like a negative image of the weights δ (Figure 7), which is obviously explained by the constraint expressed by equation (3).

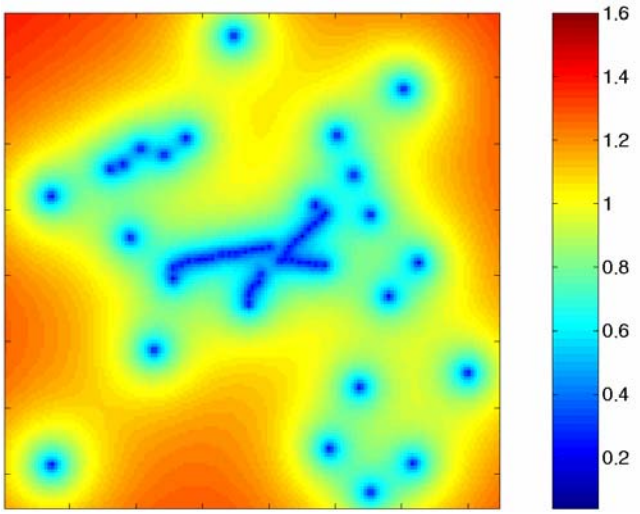

Figure 11. Kriging variance computed over the 3×3 km² Alpilles site using an exponential variogram

CONCLUSION

This paper presented the methodology used within the VALERI project for the validation of the biophysical products derived from medium resolution satellite sensors. The VALERI web site (www.avignon.inra.fr/valeri/) provides additional information on the methodological aspects as well as on the sites and their characterization. The methodology has evolved and and has currently reached a satisfactory level of maturity allowing it to be applied routinely on a large number of sites. Nevertheless, a number of critical points have been identified that still need additional investigations :

- Although many studies report the advantage of using hemispherical cameras for an improved estimation of gap fraction, no clear demonstration of the operationallity of the system has yet been done. This is a very important point, since hemispherical photographs is a convenient technique that offers the potential to account for foliage clumpiness and greeness confusion that may very significantly affect the characterization of important vegetation types (Fernandes, White et al. 2002). Attention has been paid to this critical point and measurements are currently processed to compare estimates of *LAI* based on hemispherical photos to those achieved by other classical methods (Hyer and Goetz 2004). Anyway, hemispherical photographs are certainly one of the best methods to compute the *fAPAR* values.
- The transfer function is the main process used for extending the local meaurements to the whole site. Empirical relationships generally provide the best results when the sampling by the ESUs is representative of the whole site. This confirms the importance of a well designed sampling scheme that could be based on prior information such as a previous high spatial resolution satellite image, or a land cover map. However, potential (but presumably marginal) improvements could be achieved by using enhanced transfer function types based on robust regression methods that allows to discard outliers. It is also important to include in the calibration data set, a representative sample of perfectly known objects such as bare soil, water, roads, for which no green vegetation is observed and thus *LAI*, *fAPAR* and *fCover* are nul.
- The validation activity is currently limited to the biophysical variables that could be estimated from ground measurements of the gap fraction. However, it is desirable to extend that to additional biophysical products such as the chlorophyll content and the albedo. This will require important efforts to investigate the associated spatial and temporal sampling strategies. Further, the high spatial resolution satellite images currently used for *LAI*, *fAPAR* and *fCover* might have insufficient spectral or directional sampling to establish strong enough transfer functions.
- The size of the sites is currently limited to 3×3 km², which should be enough for sensors with a spatial resolution smaller than 1 km². However, for coarser spatial resolution sensors such as MSG and POLDER, special strategies have to be developped for the validation, that will be presumably be based on extrapolation of the local measuements over the ESUs outside the 3×3 km².

The main output of such validation activity is a high spatial resolution map of the biophysical variables as derived from ground measurements and a high spatial resolution satellite image such as SPOT or TM/ETM+. This is consistent with the CEOS recommandations. We should note also that this validation activity implicitely turns to be a high spatial resolution satellite sensor product generation activity that could be used for other applications than just the validation of medium resolution satellite sensors. A consistent processing of the whole data gathered over the ensemble of sites could lead to enhance the description of the relationships between canopy radiometric response and the corresponding biophysical variables for a range of vegetation types and states.

Apart from the high spatial resolution biophysical map product, the validation exercise should also include the agregation process used to validate the medium resolution satellite sensor products. This agregation process is not straightforward when considering the associated uncertainties. Block kriging as proposed by (de Beaufort 2000) could be used to take advantage from the data available and processing already achieved. However, other sources of uncertainties have to be accounted for, including the registration errors of the medium resolution satellite sensor images that could be very significant in case of heterogeneous landscapes. Further investigations are currently directed towards the agregation problem that represents the ultimate step of the validation process. Note that the registration of the medium spatial resolution sensors to the high spatial resolution map generated should be as accurate as possible. This could be achieved by correlation techniques, and a particular module was developped for this purpose.

As stated earlier, medium resolution satellite validation activity should benefit from the contribution of worldwide distributed validation projects among which VALERI is contributing to. Concurrent use of the several validation projects will provide more reliable results. However, this requires a minimum of consistency between individual validation projects, both for the site selection and the methodological aspects, but also for the accessibility of the data and the documentation of the format used. This re-enforces the role of the Commitee on Earth Observation Satellites (CEOS) by the Working group on Calibration and Validation (WGCV), sub-group on Land Product Validation (LPV) to reach a sufficient consensus on the validation activity.

Aknowledgements. We would like to thank CNES for suporting this activity, J. Privette and J. Morisette for their chairing of the CEOS Land Product Validation group facilitating the contact and consistency with other validation activities, Boston university, particularly R. Myneni and Y. Knyazikhin for the very fruitful discussions that allowed to mature the methodology.

We would like also to thank very much all those who participated to the field campaigns, and particularly N. Bruguier, R. Olivier, J.F. Hanocq, O. Marloie, B. Combal, O. Bajoles, N. Rochdi, C. Lazar, L. Prévot, L. de Beaufort, R. Cardenas, J.L. Roujan, G. Smith, S. Rambal, Freddy Loza de la Cruz, Rufian Villca Carex, Justina Mollo de Villca. P. Hiernaux, L. Jarlan, F. Lavenu, G. Marty, P. Mazzega, Y. Tracol, B. Ruelle, S. Weber, O. Ngwété et R. Santé.

References

Buckland, S.T. and Turnock, B.J. 1992. A robust line transect method. Biometrics 48, 901-909.

Baret, F., B. Andrieu, et al. (1993). Gap fraction measurement from hemispherical infrared photography and its use to evaluate PAR interception efficiency. Crop structure and microclimate: characterization and applications. C. Varlet-Grancher, R. Bonhomme and H. Sinoquet. Paris (France), INRA edition**:** 359-372.

Baret, F., M. Weiss, et al. (2002). "VALERI: a network of sites and a methodology for the validation of land satellite products." Remote Sensing of Environment **in preparation**.

Becker, F. and Z. L. Li (1995). "Surface temperature and emissivity at various scales: definition, measurement and related problems." Remote Sensing Reviews **12**: 225-253.

Belward, A. S., J. E. Estes, et al. (1999). "The IGBP-DIS global 1 km land cover data set: a project overview." Photogrammetric Engineering and Remote Sensing **65**(9): 1013-1020.

Chen, J. M., T. A. Black, et al. (1991). "Evaluation of hemispherical photography for determining plant area index and geometry of forest stand." Agricultural and Forest Meteorology **56**: 129-143.

Chen, J. M. and J. Cilhar (1995). "Plant canopy gap-size analysis theory for improving optical measurements of leaf area index." Applied Optics **34**(27): 6211-6222.

Chen, J. M., G. Pavlic, et al. (2002). "Derivation and validation of Canada wide coarse resolution leaf area index maps using high resolution satellite imagery and ground masurements." Remote Sensing of Environment **80**: 165-184.

Cihlar, J., S. Denning, et al. (2000). IGOS-P: Carbon cycle observation theme: terrestrial and atmospheric componants., IGOS-P**:** 43.

Cilhar, J., A. S. Denning, et al. (2000). Global terrestrial carbon observation: requirements, present status and next steps. Ottawa (Canada), GTOS**:** 101.

de Beaufort, L. (2000). Définition d'une méthode de cartographie d'indice foliaire destinée à la validation des produits de capteurs à large champ. Avignon, INRA Bioclimatologie**:** 84.

De Fries, R. S., J. R. Townshend, et al. (1997). Scaling land cover heterogeneity for global atmosphere-biosphere models. Scales in Remote Sensing and GIS. D. A. Quattrochi and M. F. Goodrich. Boca Raton, Florida, USA, CRC Press**:** 231-246.

Duchemin, B., B. B., et al. (2002). "Normalisation of directional effects in 10-day global syntheses derived VEGETATION/SPOT I. Validation of an operational method on actual data sets." Remote Sensing of Environment **81**(101-113).

Fernandes, R., C. Burton, et al. (2003). "Landsat-5 TM and Landsat-7 ETM+ based accuracy assessment of leaf area index products for Canada derived from SPOT-4 VEGETATION data." Canadian Journal of Remote Sensing. **20**(2): 241-258.

Fernandes, R., H. P. White, et al. (2002). "Examination of error propagation in relationships between leaf area index and spectral indices from Landsat TM and ETM." draft.

Gond, V., D. G. G. de Pury, et al. (1999). "Seasonal variation in leaf area index, leaf chlorophyll, and water content; scaling up to estimate fAPAR and carbon balance in a multilayer, multispecies temperate forest." Tree Physiology **19**: 673-679.

Goovaerts, P. (1997). Geostatistics for Natural Ressources Evaluation. Oxford (UK), Oxford University Press.

Heal, O. W., J.-C. Menaut, et al. (1995). Towards a Global Terrestrial Observing System (GTOS): Detecting and Monitoring Change in Terrestrial Ecosystems,, IGBP.

Hyer, E. J. and S. J. Goetz (2004). "Comparison and sensitivity analysis of instruments and radiometric methods for LAI estimation: assessments from a boreal forest site." Agriculture and Forest Meteorology **122**: 157-174.

Jacob, F., M. Weiss, et al. (2002). "Assessing the narrowband to broadband conversion to estimate visible, near infrared and shortwave apparent albedo from airborne POLDER." Agronomie **22**: 537-546.

Jacquemoud, S. and F. Baret (1990). "PROSPECT: A model of leaf optical properties spectra." Remote Sensing of Environment **34**: 75-91.

Justice, C., A. Belward, et al. (2000). "Developments in the validation of satellite sensor products for the study of the land surface." International Journal of Remote Sensing **21**(17).

Justice, C. O., D. Starr, et al. (1998). "EOS land validation coordination: an update." Earth Observer **10**: 55–60.

Leblanc, S., R. Fernandes, et al. (2002). Recent advancements in optical field leaf area index, foliage heterogeneity, and foliage angular distribution measurements. IGARSS 02.

Liang, S., C. J. Shuey, et al. (2002). "Narrowband to broadband conversions of land surface albedo: II Validation." Remote Sensing of Environment **84**: 25-41.

Loveland, T. R., B. C. Reed, et al. (2000). "Development of a global land cover characteristics database and IGBP DISCover from 1 km AVHRR data." International Journal of Remote Sensing **21**(6): 1303-1330.

Malingreau, J. P. and A. S. Belward (1992). "Scale considerations in vegetation monitoring using AVHRR data." International Journal of Remote Sensing. **13**(12): 2289-2307.

Martonchik, J. V. (1994). "Retrieval of surface directional reflectance properties using ground level multiangle measurements." Remote Sensing of Environment **50**: 303-316.

Morissette, J., J. Privette, et al. (2000). MODIS land validation activities: status and review. IGARS'2000, Honolulu.

Myneni, R. B., C. D. Keeling, et al. (1997). "Increased plant growth in the Northern high latitudes from 1981-1991." Nature **386**: 698-702.

(NOAA), N. O. a. A. A. (1997). Climate Measurement Requirements for the National Polar-orbiting Operational Environmental Satellite System (NPOESS), Office of Research and Applications, National Environmental Satellite, Data, and Information Service, National Oceanic and Atmospheric Administration**:** 77.

Privette, J., R. Myneni, et al. (1998). "Global validation of EOS and FPAR products." The Earth Observer **10**(6): 39-42.

Privette, J. L., J. Morisette, et al. (2001). " Summary of the International Workshop on LAI Product Validation." Earth Observer **13**(3): 18-22.

Raffy, M., K. Soudani, et al. (2003). "On the variability of the LAI of homogeneous covers with respect to surface size and application." International Journal of Remote Sensing **24**(10): 2017-1035.

Tian, Y., C. E. Woodcock, et al. (2002). "Multiscale analysis and validation of the MODIS LAI product I. Uncertainty assessment." Remote Sensing of Environment **83**: 414-430.

Tian, Y., C. E. Woodcock, et al. (2002). "Multiscale analysis and validation of the MODIS LAI product II. Sampling strategy." Remote Sensing of Environment **83**: 431-441.

Verhoef, W. (1984). "Light scattering by leaf layers with application to canopy reflectance modeling: the SAIL model." Remote Sensing of Environment **16**: 125-141.

Verhoef, W. (1985). "Earth observation modeling based on layer scattering matrices." Remote Sensing of Environment **17**: 165-178.

Wackernagel, H. (1995). Multivariate geostatistics, an introduction with applications, Springer Verlag.

Wanner, W., A. H. Strahler, et al. (1997). "Global retrieval of bidirectional reflectance and albedo over land from EOS MODIS and MISR data: theroy and algorithm." Journal of Geophysical Research **102**: 17143-17162.

Weiss, M., F. Baret , et al. (2002). "Validation of neural net techniques to estimate canopy biophysical variables from remote sensing data." Agronomie **22**: 547-554.

Weiss, M., F. Baret, et al. (2000). Validation of neural network techniques for the estimation of canopy biophysical variables from VEGETATION data. VEGETATION preparatory programme. Final meeting, Belgirate (Italy), G. Saint.

Weiss, M., F. Baret, et al. (2000). "Investigation of a model inversion technique for the estimation of crop charcteristics from spectral and directional reflectance data." Agronomie **20**: 3-22.

Weiss, M., F. Baret, et al. (2004). "Review of methods for in situ leaf area index determination, part II: Estimation of LAI, errors and sampling." Agricultural and Forest Meteorology **121**: 37-53.